Smart Structures and Systems, Vol. 5, No. 4 (2009) 345-355 345
DOI: http://dx.doi.org/10.12989/sss.2009.5.4.345

Serially multiplexed FBG accelerometer for structural health monitoring of bridges

I. Talebinejad, C. Fischer and F. Ansari*

Smart Sensors & NDT Laboratory, Civil and Materials Engineering Dept., University of Illinois at Chicago, Chicago, IL 60607, U.S.A.

(Received August 18, 2008, Accepted September 21, 2008)

Abstract. This article describes the development of a fiber optic accelerometer based on Fiber Bragg Gratings (FBG). The accelerometer utilizes the stiffness of the optical fiber and a lumped mass in the design. Acceleration is measured by the FBG in response to the vibration of the fiber optic mass system. The wavelength shift of FBG is proportional to the change in acceleration, and the gauge factor pertains to the shift in wavelength as a function of acceleration. Low frequency version of the accelerometer was developed for applications in monitoring bridges. The accelerometer was first evaluated in laboratory settings and then employed in a demonstration project for condition assessment of a bridge. Laboratory experiments involved evaluation of the sensitivity and resolution of measurements under a series of low frequency low amplitude conditions. The main feature of this accelerometer is single channel multiplexing capability rendering the system highly practical for application in condition assessment of bridges. This feature of the accelerometer was evaluated by using the system during ambient vibration tests of a bridge. The Frequency Domain Decomposition method was employed to identify the mode shapes and natural frequencies of the bridge. Results were compared with the data acquired from the conventional accelerometers.

Keywords: accelerometers; bridges; Fiber Bragg Gratings (FBG); Structural Health Monitoring (SHM).

1. Introduction

Vibration based structural health monitoring (SHM) methods employ the natural frequencies and mode shapes for detection of damage in structures. Examples include methods primarily based on changes in the natural frequencies (Cawley and Adams 1979, Salawu 1997), mode shape curvatures (Pandey, *et al.* 1991), flexibility coefficients derived from modal properties (Pandey and Biswas 1994), stiffness coefficients derived from modal properties (Zimmerman and Kaouk 1994) and changes in the curvature of the uniform load surface derived from modal properties (Zhang and Aktan 1995). In general, accelerometers are strategically placed in bridges for extraction of dynamic characteristics. While, the conventional PZT based accelerometers have served the purpose well, there has been a surge in interest on other sensor types, in particular fiber optic Bragg gratings. The obvious advantages of optical fiber sensors are immunity to electrical and electromagnetic interferences, high resolution, and geometric compatibility. From practical point of view, especially for applications in bridges, single channel serial multiplexing of optical fibers reduces the amount of wiring that is required for acquisition of data (Ansari 2007). The individual accelerometers are connected in series by way of conventional

*Corresponding Author, E-mail: fansari@uic.edu

optical fiber connectors. This allows for easy exchange of accelerometers in case of malfunction.

Review of technical literature reveals that concerted efforts for development of fiber optic based sensing of acceleration did not begin until the mid-1990s. Berkoff and Kersey (1996) proposed an accelerometer consisting of a mass laid on a commercially available compliant material which acted like a spring and sandwiched in between rigid plates. The wavelength shift of the FBG embedded in the compliant material was calibrated against acceleration. This sensor exhibited sensitivity to cross-axis excitation. Storgaard-Larsen, *et al*. (1996) presented a micro opto-mechanical accelerometer with FBG as sensing element. This sensor exhibited high sensitivity and a wide dynamic range. it was rather complex in construction. Todd, *et al*. (1998) proposed an FBG accelerometer consisting of dual flexural beams and a seismic mass welded in between the beams. This sensor had low cross-axis sensitivity with a resonant frequency of 1 KHz. In general, broadening of reflected wavelength peaks due to nonuniformity of strains along the length of the cantilever reduces the resolution of measured acceleration. To avoid peak broadening, in Mita and Yokoi design which was also cantilever based, the FBG was not directly adhered to the beam (2000). In another cantilever based design, the peak broadening was avoided by inducing a state of uniform strain along the length of a triangular beam (Shi, *et al*. 2003). In another study, Teng, *et al*. (2006) designed an accelerometer which was a combination of a larger beam and two smaller ones.

This article describes results of a research pertaining to the development of a low frequency FBG based accelerometer. The accelerometer utilizes the stiffness of the optical fiber and a lumped mass in the design. This design alleviates the peak broadening issues inherent of cantilever based systems. Acceleration is measured by the FBG in response to the vibration of the fiber optic mass system. The main feature of this accelerometer is single channel multiplexing capability rendering the system highly practical for application in condition assessment of bridges. This feature of the accelerometer was evaluated by using the system in structural health monitoring of a bridge. The Frequency Domain Decomposition method was employed to identify the mode shapes and natural frequencies of the bridge. The sensor concept and accelerometer design is described next.

2. Sensor concept and accelerometer design

The basic principle behind the proposed accelerometer design is that of a mass – spring system consisting of the spring which in this case is a taut optical fiber and the lumped mass. The optical fiber vibrates when displaced in transverse direction (Fig. 1), and the motion is simply given by:

$$a = \frac{Kx}{M} \tag{1}$$

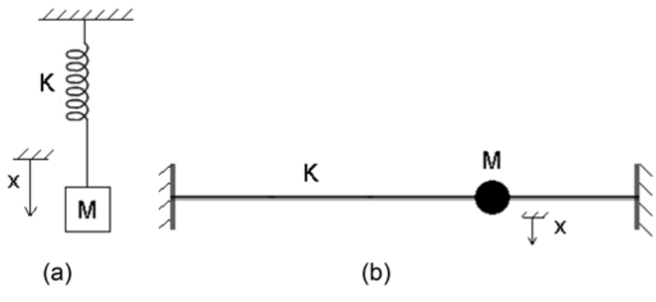

Fig. 1 (a) Spring-mass system, (b) Fiber optic lumped mass system

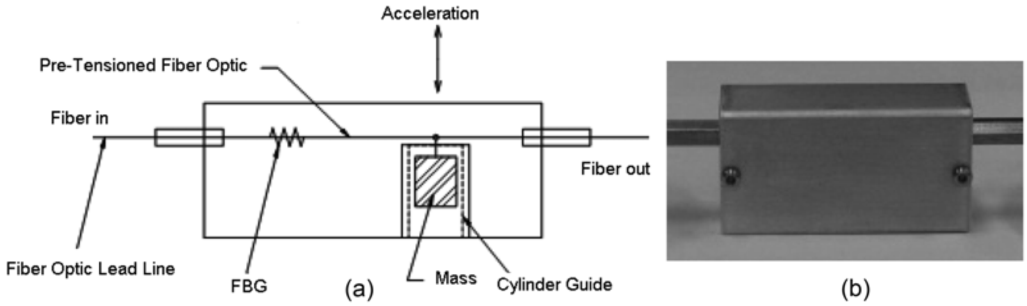

Fig. 2 (a) schematic design of the FBG accelerometer, (b) photo of the FBG accelerometer

Where, a is acceleration, K is the spring constant, M is mass, and x is the spring's displacement. This approach was taken in order to avoid the wavelength peak broadening of the FBG which is common in cantilever beam designs.

The accelerometer design follows this simple concept, and as shown in Fig. 2, the optical fiber with FBG is stretched by a predetermined amount to achieve the required spring constant per accelerometer requirements. A lumped mass is attached to the fiber and guided through a precisely machined tube in order to eliminate the cross axis sensitivity.

This approach is verified numerically and the basic parameters of the system, i.e. tension in the fiber and the lumped mass are selected according to the desired fundamental frequency of the accelerometer. Finite element approach is used to acquire the design spring constant and the lumped mass based on the required fundamental frequency. For a given material properties and the designed dimensions of the accelerometer linear modal analysis was performed to extract the natural frequency of the system. The parameters employed for the design of the prototype accelerometer are given in Table 1. The analysis was performed to achieve a fundamental frequency of 50 Hz. Based on the parameters given in Table 1, the finite element results yielded a fundamental frequency of 52.5 Hz. These parameters were then employed for the fabrication of the accelerometer yielding 50 Hz for the fundamental frequency yielding approximately a 4.8 percent error between the computed and measured fundamental frequencies of the accelerometer. Fig. 3 corresponds to the finite element model and the mode shape of the fiber optic-lumped mass accelerometer.

3. Sensor calibration and basic experiments

The basic principle of an FBG based sensor system lies in the monitoring of the wavelength shift of the returned Bragg-signal as a function of the measurand, in this case is acceleration. The calibration process was accomplished by mounting the FBG accelerometer along with a high-precision conventional piezoelectric accelerometer of known sensitivity on the cantilever beam. The wavelength shift due to the acceleration was measured during the experiments involving induced vibration of the beam. The gauge factor for the FBG accelerometer was determined by the following equation:

Table 1 Design parameters of the accelerometer

Mass (kg)	E_G (GPa)	T (N)	ρ (kg/m^3)	L (m)
0.005	80	6.2	100	0.06

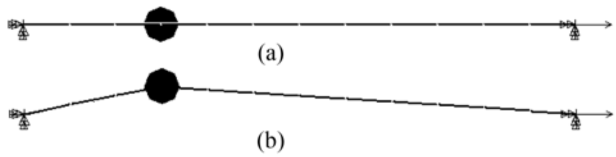

Fig. 3 (a) Finite element model of the sensor, (b) Fundamental mode of the sensor vibration

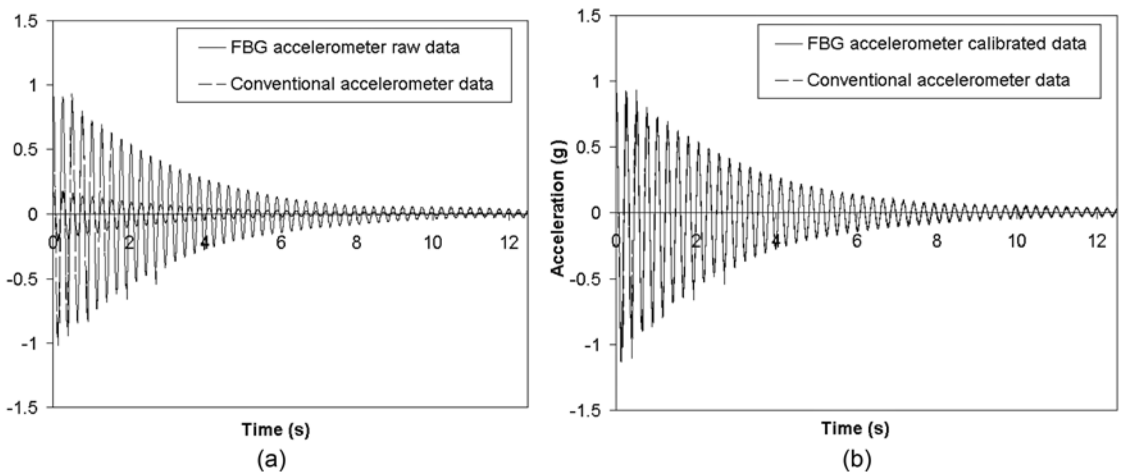

Fig. 4 FBG accelerometer raw data (a) and calibrated data (b) vs. conventional accelerometer data

$$G = \frac{\Delta\lambda/\lambda}{a} \tag{2}$$

where G = gage factor, $\Delta\lambda$ = change in wavelength, λ = wavelength, and a = acceleration measured by the conventional accelerometer. Fig. 4(a) corresponds to a typical raw data from FBG accelerometer which is compared with the output of the conventional PZT accelerometer. The amplitudes of both sensors are in-sync and therefore it is possible to calibrate the FBG against PZT, and therefore Eq. (2) was employed for computing the gauge factor by relating the wavelength shift of the optical fiber to the acceleration measured by the conventional accelerometer. The calibrated results comparing the optical fiber and the PZT accelerometer data are shown in Fig. 4(b).

A series of experiments were performed to determine the resolution and the minimum detectable frequency of the proposed FBG accelerometer. In these experiments a closed-loop servo-hydraulic actuator was employed with capability to induce pre-determined sinusoidal displacements of known frequencies. The optical fiber accelerometer was mounted on the hydraulic actuator and it was subjected to a series of sinusoidal displacements with known frequencies and a range of amplitudes (Fig. 5).

The experiments involved a frequency range of 0.1-0.6 Hz with amplitudes varying gradually until the applied frequency was detectable by the FBG accelerometer. Comparison of the measured and applied results is shown in Table 2. As shown in Table 2, the proposed FBG accelerometer is capable of sensing frequencies as small as 0.2 Hz with an average resolution of 0.015 g. A sensor sensitivity of about 0.2 nm/g was acquired for the designed accelerometer.

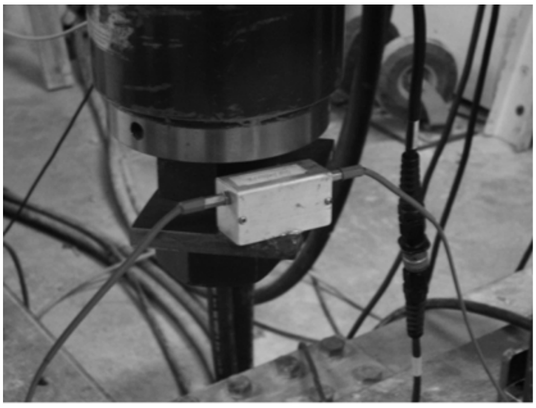

Fig. 5 Fiber optic accelerometer mounted on the hydraulic jack

Table 2 Applied and measured frequencies and amplitudes recorded by FBG accelerometer

Applied frequency	Measured frequency	Error (%)	Applied amplitude (%g)	Average measured amplitude (%g)	Error (%)
0.1	-	-	-	-	-
0.2	0.198	1	0.017	0.018	-5.8
0.3	0.298	0.5	0.015	0.015	0
0.4	0.397	0.75	0.015	0.015	0
0.5	0.499	0.2	0.015	0.015	0
0.6	0.610	-1.7	0.012	0.013	-8

4. Bridge tests

The serial multiplexing capabilities and performance of the FBG accelerometers were verified by using them to monitor the vibrations of a full scale bridge. The bridge used in this study was a single span slab on girders located in a western suburb of Chicago, Illinois (Fig. 6). The bridge, originally constructed in 1924 is 20.27 meter long. The superstructure consisted of eight reinforced concrete

Fig. 6 Photograph of bridge

beams spaced at 1.98 m on center with 1.07 m overhangs on each side. The bridge has an overall width of 16.00 m. The beams were supported on fixed bearings at the west end and rockers at the east end. The concrete slab had a thickness of 203 mm with an additional concrete wearing surface of 101 mm.

The bridge carried two lanes of traffic in each direction and there was a narrow sidewalk on either side of the bridge. Since the bridge was not closed to traffic during monitoring, the sensors were installed on both sides of the bridge over the outer beams located under the sidewalks. The traffic on the bridge consisted of a mix of trucks and cars. The speed limit on the road over the bridge was 72 km/hr. The traffic loading was more than sufficient to dynamically excite the bridge. The vibrations of the bridge due to traffic could be felt by standing in the middle sections of the bridge. There was an expansion joint at each end of the bridge. The expansion joint on the west end of the bridge was raised approximately 30 mm above the pavement causing the traffic going over the hump that created additional dynamic loads.

4.1. Numerical modeling of the bridge

Prior to the field testing of the bridge it was modeled using a commercial finite element program (ANSYS) in order to extract the modal properties and comparison with the experimental results. The bridge was modeled using Solid 90 elements with the material properties shown in Table 3.

Supports were assumed to be fixed bearing at one end and roller at the other end. The geometry of the bridge resembled that of a plate supported on two ends. Consequently, some combinations of bi-directional bending mode shapes were identified in the numerical model. For instance, the third mode is the first coupled bending mode shape of the bridge in the longitudinal and transverse directions. The computed natural frequencies of the bridge are shown in Table 4. The first bending and torsional mode shapes of the bridge are shown in Fig. 7, whereas, the first and second coupled bending mode shapes are given in Fig. 8.

4.2. Instrumentation and modal analysis of the bridge

The bridge remained open to traffic during the tests and therefore the accelerometers were mounted on the sidewalks. There were eight optical fiber accelerometers available and therefore, they were serially multiplexed 4 per line for the opposing sides of the bridge across the traffic lanes. This configuration only required two channels of data acquisition and two optical fiber lead lines for the eight accelerometers. Fig. 9 is the schematics corresponding to the location of the accelerometers on the bridge.

Table 3 Material properties of the deck concrete

Modulus of elasticity (MPa)	Poisson's ratio	Density (Kg/m^3)
29647	0.2	2400

Table 4 Numerical frequencies of the bridge

Mode number	Numerical natural frequencies	Mode specification
1	10.64	Vertical Bending
2	11.12	Torsional
3	13.12	Coupled bending
4	17.07	Coupled bending

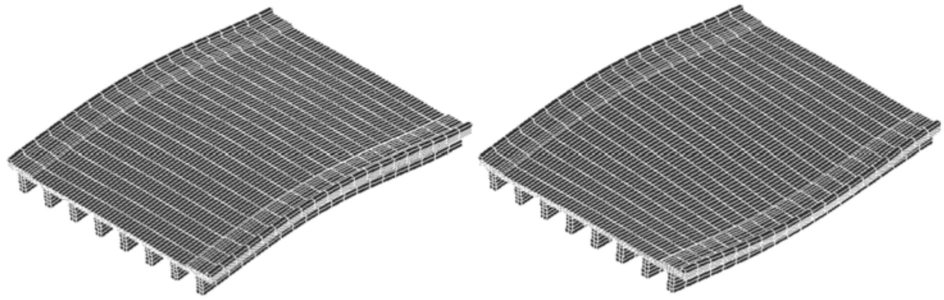

Fig. 7 First bending and torsional mode shapes

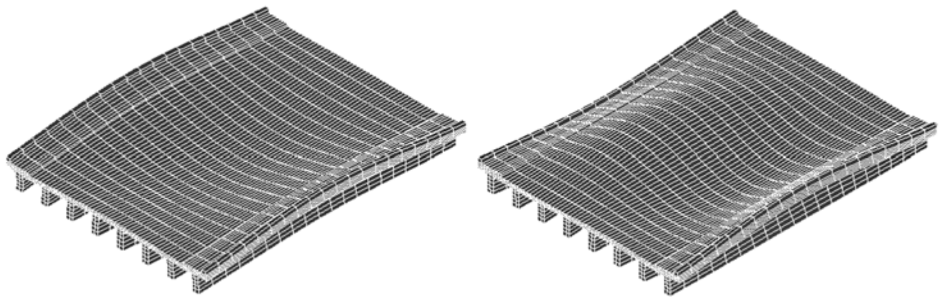

Fig. 8 First and second coupled bending mode shapes

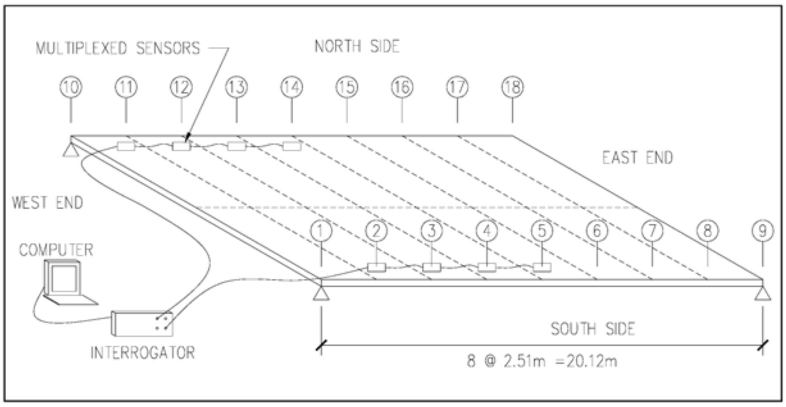

Fig. 9 Accelerometer locations on the bridge

To cover the entire length of the bridge corresponding to the fourteen sensing points (nodes 2-8 and 11-17) shown in Fig. 9, the eight sensors were placed at nodes 2 through 5 as well as nodes 11 through 14 and following the acquisition of data sequentially moved to the next set of sensing points. The measurements at locations 4 and 13 in Fig. 9 were used as fixed reference response signals. This sensor configuration allowed for the acquisition of the first bending and first torsional mode shapes of the bridge. Eight PCB piezoelectric accelerometers with the sensitivity of 1000 mv/g were also employed for comparison with the fiber optic accelerometers. The data acquisition setup included a computer, and eight channel data acquisition board, and the fiber optic interrogation unit (Micron Optics SI 425). Data was acquired at a sampling rate of 250 Hz for both systems. A portable generator was used to provide power for the measurement systems.

4.3. Frequency domain decomposition method

The bridge was monitored under ambient traffic conditions and identification of the modal properties of the bridge was accomplished by an output only algorithm. The classical approach to determine the modal parameters of output-only systems is to use a frequency domain approach such as peak picking. Frequency Domain Decomposition (FDD) is closely related to the peak picking approach but allows modes that are close in natural frequency to be identified with greater accuracy. Although a complete description of theoretical basis for FDD method is given by Brinker, *et al*. (2001), a brief review is presented here for completeness.

The relationship between the unknown inputs x(t) and the measured response y(t) can be expressed as:

$$G_{yy}(j\omega) = \bar{H}(j\omega)G_{xx}(j\omega)H(j\omega)^T \tag{3}$$

where $G_{xx}(j\omega)$ is the Power Spectral Density (PSD) matrix of the input, $G_{yy}(j\omega)$ is the PSD matrix of the responses, $H(j\omega)$ is Frequency Response Function (FRF) matrix. If the input is white noise and the damping is light, this equation can be written as:

$$G_{yy}(j\omega) = \sum \frac{d_k\phi_k\phi_k^T}{j\omega-\lambda_k} + \frac{\bar{d}_k\bar{\phi}_k\bar{\phi}_k^T}{j\omega-\bar{\lambda}_k} \tag{4}$$

This is a modal decomposition of the spectral matrix. For the FDD method, the PSD matrix of the output response is decomposed by taking the singular value decomposition (SVD).

$$\hat{G}_{yy}(j\omega_i) = U_iS_{+i}U_i^H \tag{5}$$

where the matrix $U_i = [u_{i1}, u_{i2},...,u_{in}]$ is a unitary matrix holding the singular vectors u_{ij}, and S_i is a diagonal matrix holding the scalar singular values s_{ij}. Comparing Eqs. (4) and (5), mode shapes of the structures are estimated using these singular vectors.

4.4. Natural frequencies and mode shapes of the bridge

The power spectra were computed on the basis of multi averages of data allowing a 50% overlap between the different data blocks. A Hanning window with a length of 8000 points was used to reduce leakage errors. A bandpass butterworth filter was applied to the raw data obtained from both conventional and FBG accelerometers to remove the undesired portion of the signal. Figs. 10(a) and (b) show the Power Spectral Density (PSD) diagram for one of the FBG accelerometer sensors and its corresponding conventional accelerometer. As can be seen, the first and second natural frequencies of the bridge have been detected by both sensor types. As all the accelerometers installed on the sides of the bridge, the third and fourth experimental mode shape can not be acquired. So, the third frequency peak in both PSD diagrams and fourth one in the FBG PSD diagram are not verified to be the third and fourth natural frequencies. Therefore, these peaks are just considered as two natural frequencies of the bridge.

The peak around 50 Hz in PSD diagram of FBG accelerometer is related to the natural frequency of the FBG accelerometer itself. Table 5 shows the natural frequencies acquired from both conventional and FBG accelerometers as well as the numerical analysis. The maximum error between the measurements by the FBG and conventional accelerometers is 0.8 percent. Comparing the natural frequencies from experimental data with numerical model, a maximum difference of 22 percent is observed for the

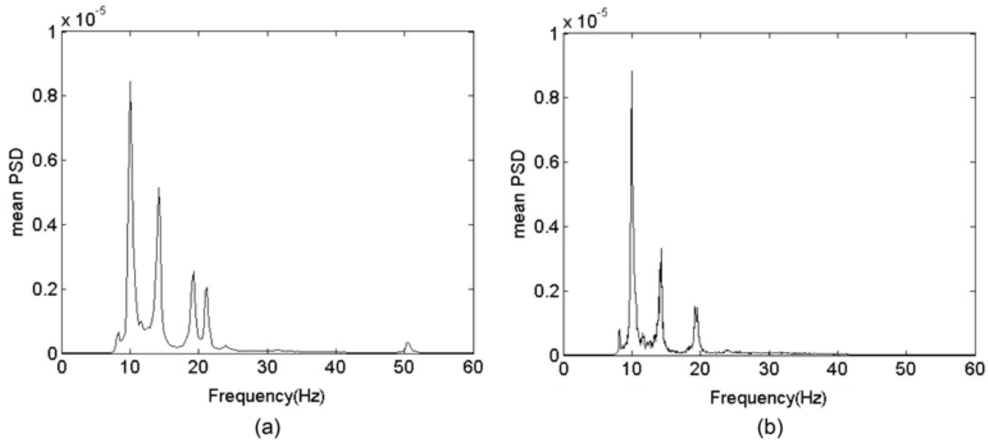

Fig. 10 PSD diagram for (a) FBG accelerometer and (b) conventional accelerometer

Table 5 Natural frequencies of the bridge

Mode number	Experimental natural frequencies		Error (percent)	Numerical natural frequencies	Error (percent)
	FBG	Conventional			
1	10.01	10.01	0	10.64	6
2	14.16	14.28	0.8	11.12	22
3	19.28	19.19	0.5	-	-
4	21.24	-	-	-	-

second mode. Results obtained by the finite element model exhibit high sensitivity to the boundary condition of the supports, and the model should be tuned. For instance, some rotational fixity might exist at the beams' supports (west end) where they are attached to the abutment. Numerical analysis indicated that this will increase the first and second frequencies of the bridge to 11.4 and 12.1 Hz, respectively. In this case, the percent increase for the first and second modes of vibration for the bridge are 12 and 9 percent respectively.

The FDD identification method was used to extract the modal properties of the bridge from ambient vibration data. Figs. 11 and 12 correspond to the estimated mode shapes from both the FBG and conventional accelerometers. The Modal Assurance Criteria (MAC), a widely used technique to estimate the degree of correlation between mode shape vectors, was used to correlate the data

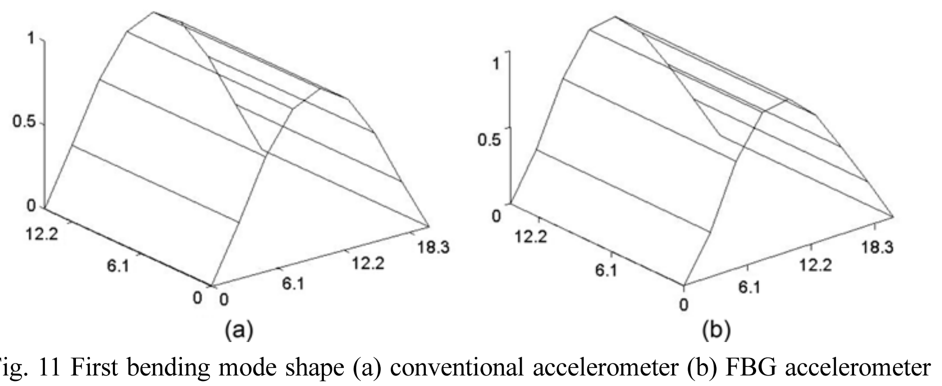

Fig. 11 First bending mode shape (a) conventional accelerometer (b) FBG accelerometer

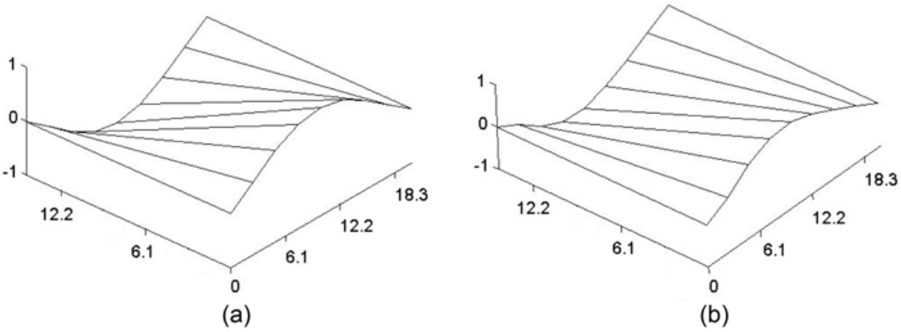

Fig. 12 First torsional mode shape (a) conventional accelerometer (b) FBG accelerometer

(Allemang and Brown 1982). The MAC between a mode vector ϕ_{mj} and mode vector ϕ_{ak} is defined as:

$$MAC_{jk} = \frac{\left|\phi_{mj}^{T}\phi_{ak}\right|^{2}}{(\phi_{ak}^{T}\phi_{ak})(\phi_{mj}^{T}\phi_{mj})} \tag{6}$$

The MAC value of 99% was obtained for both first bending and torsional mode shapes showing a good correlation between the FBG and conventional accelerometer data.

5. Conclusions

Development of a fiber optic accelerometer based on Fiber Bragg Gratings (FBG) is described in this article. Utilization of the optical fiber as the spring element in a mass spring setup eliminated the peak broadening issues in FBG inherent of cantilever beam based designs. The accelerometer utilizes the stiffness of the optical fiber and a lumped mass in the design. Design parameters for the accelerometer were selected through finite element modeling of the system. Evaluation of the accelerometer in the laboratory involved application of pre-determined sinusoidal displacements of known frequencies and a range of amplitudes. This accelerometer has a resonant frequency of 50 Hz, sensitivity of 0.2 nm/g and resolution of 0.015 g. The lower limit frequency detection limit of this accelerometer is 0.2 Hz. The main feature of this accelerometer is single channel multiplexing capability rendering the system highly practical for application in condition assessment of bridges. This feature of the accelerometer was evaluated by using the system during ambient vibration tests of a bridge. First and second natural frequencies and mode shapes of the bridge were extracted and compared with the finite element model and conventional PZT accelerometers. Results were comparable. The controlling factor for the design of the accelerometer is the tension in the optical fiber that can be adjusted to design other versions of this system for other frequency requirements.

Acknowledgements

The work described here was supported by a grant from the National Science Foundation, grant number 0730259. The financial support by NSF is greatly appreciated.

References

Allemang, R.J. and Brown, D.L. (1982), "A correlation coefficient for modal vector analysis", *1st Int. Modal Analysis Conf.*, Orlando, November.

Ansari, F. (2007), "Practical implementation of optical fiber sensors in civil structural health monitoring", *J. Intel. Mat. Syst. Str.,* **18**, 879-889.

Berkoff, T.A. and Kersey, A.D. (1996), "Experimental demonstration of a fiber bragg grating accelerometer", *IEEE Photonics Tech. L.*, **8**, 1677-1679.

Brincker, R., Zhang, L. and Andersen, P. (2001), "Modal identification of output-only systems using frequency domain decomposition", *Smart Mater. Struct.,* **10**, 441-445.

Cawley, P. and Adams, R.D. (1979), "The location of defects in structures from measurements of natural frequencies", *J. Strain Anal. Eng.*, **14**(2), 49-57.

Mita, A. and Yokoi, I. (2000), "Fiber bragg grating accelerometer for structural health monitoring", *Fifth Int. Conf. on Motion and Vibration Control* (MOVIC 2000), Sydney, December.

Pandey, A.K., Biswas, M. and Samman, M.M. (1991), "Damage detection from changes in curvature mode shapes", *J. Sound Vib.*, **145**, 321-332.

Pandey, A.K. and Biswas, M. (1994), "Damage detection in structures using changes in flexibility", *J. Sound Vib.*, **169**(1), 3-17.

Salawu, O.S. (1997), "Detection of structural damage through changes in frequency: a review", *Eng. Struct.*, **19**(9), 718-723.

Shi, C.Z., Zeng, N., Ho, H.L., Chan, C.C., Zhang, M., Jin, W. and Liao, Y.B. (2003), "Cantilever optical vibrometer using fiber Bragg grating", *Opt. Eng.*, **42**, 3179.

Storgaard-Larsen, T., Bouwstra, S. and Leistiko, O. (1996), "Opto-mechanical accelerometer based on strain sensing by a Bragg grating in a planar waveguide", *Sensors Actuat.*, **A52**, 25-32.

Teng, L., Feng, L., Lin, H., Zhang, B. and Liu, C. (2006), "A new fiber Bragg grating accelerometer", *Proc. SPIE*, **6357**, 63574C.

Todd, M.D., Johnson, J.A., Althouse, B.A. and Vohra, S.T. (1998), "Flexural beam-based fiber bragg grating accelerometers", *IEEE Photonics Tech. L.*, **10**, 1605-1607.

Zhang, Z. and Aktan, A.E. (1995), "The damage indices for the constructed facilities", *Proc. 13th Int. Modal Analysis Conf.*, **2**, 1520-1529.

Zimmerman, D.C. and Kaouk, M. (1994), "Structural damage detection using a minimum rank update theory", *J. Vib. Acoust*., **116**, 222-231.